Review

Novel Materials for Semi-Transparent Organic Solar Cells

Muhammad Azhar Ansari * , **Giovanni Ciampi** * and **Sergio Sibilio**

Department of Architecture and Industrial Design, University of Campania Luigi Vanvitelli, Via San Lorenzo 4, 81031 Aversa, CE, Italy; sergio.sibilio@unicampania.it
* Correspondence: muhammadazhar.ansari@unicampania.it (M.A.A.); giovanni.ciampi@unicampania.it (G.C.)

Abstract: The rapid development of photovoltaic technology has driven the search for novel materials that can improve the cost-effectiveness and efficiency of solar cells. Organic semiconductors offer unique optical tunability and transparency, allowing customization for the absorption of specific optical spectra like near-infrared radiation. Through the molecular engineering of electron donors and acceptors, these materials can be optimized for targeted optical selectivity. This adaptability enables the development of efficient energy-harvesting devices tailored for specific spectral regions. Consequently, organic semiconductors present a promising avenue for specialized applications such as semi-transparent organic solar cells. This review offers a detailed summary of the latest developments in novel organic semiconductor materials, focusing on design principles and synthesis of materials in the context of semi-transparent organic solar cells. Optimization of molecular architecture, photovoltaic performance, and the optoelectronic properties of these materials has been explored, highlighting their potential for next-generation solar energy conversion.

Keywords: semi-transparent organic solar cells (OSCs); advanced energy materials; power conversion efficiency (PCE); near-infrared radiation (NIR)

1. Introduction

In the modern era, the world is grappling with intensifying environmental issues alongside a growing demand for sustainable energy solutions [1–4]. Solar energy, a clean and inexhaustible resource, stands at the forefront of resolving these challenges [5,6]. High-performance photovoltaic technologies have the potential to not only substantially augment global energy production but also to lessen environmental impacts [7]. In the past few years, there has been remarkable advancement in power conversion efficiency (PCE) for various solar cell technologies. Some of the record PCEs are 26.7% for mono-crystalline silicon [8], 24.4% for multi-crystalline silicon [9], 10.3% for hydrogenated amorphous silicon (a-Si:H) [10], 23.6% for CIGS [11], 22.3% for CdTe [12], 26.1% for Perovskite-single junction [13], 33.7% for Perovskite-2 Terminal (perovskite/Si) tandem solar cells [13], 20.6% for organic solar cells (OSCs) [14–16], and 14.2% for dye-sensitized solar cells [17]. Despite these advances, silicon-based photovoltaics (PV) currently dominates the market, accounting for around 95% of total commercial production. This dominance suggests that there is ample room to enhance and expand alternative PV technologies. Among various PV technologies, organic photovoltaics (OPV) emerges as a particularly promising innovation characterized by solution-based processing methods, semi-transparency, lightweight attributes, flexibility, and optical tuneability by molecular engineering [18]. OPV offers a versatile approach to solar energy conversion. In recent years, OPV technologies have witnessed groundbreaking advances, propelling their PCE above the 20% mark [14]. This impressive achievement is largely due to advances in organic semiconductor materials and device architectures. Unlike their silicon-based counterparts, which often require specialized conditions for installation, OPV devices offer greater semi-transparency, which makes them more adaptable for integration with other applications [19,20] With their unique capability for optical semi-transparency, organic semiconductors have led to the

advent of specialized OSCs that are not just confined to traditional power generation but have versatile applications, extending from Building-Integrated Photovoltaics (BIPV) to car shelters, greenhouses, automobile sunroofs, and even wearable electronics, which can be seamlessly integrated into windows, rooftops, and façades, generating electricity and contributing to the aesthetics of the built environment as well [20,21].

The notable potential of organic semiconductors is their optical tunability feature and hence transparency, which allows for targeted optical selectivity to specific spectral ranges—ultraviolet (UV), visible, or near-infrared (NIR)—through molecular engineering of the active materials, such as electron donors and electron acceptors. This tunability paves the way for customized, efficient energy-harvesting materials for specific spectral regions [22]. In contrast to the UV-visible range, the IR absorption spectrum encompasses a notable 52% of the solar spectrum's total energy. The IR spectrum can be broadly categorized into three segments: NIR, mid-IR, and far-IR. The energy of photons within the IR range varies from 1.6 to 0.025 eV, which is considerably lower than that of photons in the UV-visible region. As a result, capturing these plentiful yet lower-energy IR photons can enhance the short-circuit current density (Jsc) and, hence, the performance of OSCs [23].

There are mainly two active materials in OPV devices: electron donor materials and electron acceptor materials. The significance of donor materials in the active layer cannot be overstated, especially when considering their impact on a device's optoelectronic properties. Earlier-developed donor materials, such as P3HT polymers, were chiefly designed to absorb visible light [24,25]. However, as over half of the Sun's energy is in the IR region, there is a growing focus on capturing this untapped energy through NIR-active materials to boost PCE and transparency in the visible region. Generally, the ability to absorb NIR light is achieved by judiciously modifying the electron-donating and electron-withdrawing groups of active materials. Ideally, the most efficient materials match a potent electron donor with a complementary, strong electron acceptor, enhancing the intermolecular charge transfer (ICT) and diversifying the optical absorption profile [23,26–30]. The spotlight in OPV research has also focused on Non-Fullerene Acceptors (NFAs) and Small-Molecule Acceptors (SMAs), primarily because of their edge over traditional fullerene-based materials in several aspects. These include their tunable optical absorption, flexible energy levels, high absorption coefficients, and controllable crystallinity, not to mention lower energy loss [23,31–33]. The molecular structures of recently developed novel donor and acceptor materials in the context of ST-OSCs are shown in Figures 1 and 2, respectively. The optoelectronic properties and performance of these novel materials will be discussed in this review.

In 2020, the global BIPV market was worth USD 14.4 billion, and it is expected to grow at a Compound Annual Growth Rate (CAGR) of about 20.0% from 2021 to 2028, reaching an estimated value of USD 59.5 billion by 2028 [20]. However, the BIPV market is inaccessible to conventional OSCs because they incorporate non-transparent materials. For example, for window applications, transparency is a crucial factor. To penetrate this market, it is crucial to develop semi-transparent active-layer OSC materials in the visible region by focusing particularly on materials with enhanced absorption in the NIR region. These highly efficient materials' bandgap should be narrowed by molecular engineering to utilize a high fraction of the solar spectrum, such as NIR, to fabricate semi-transparent OSCs [22,34–36].

Therefore, this review aims to summarize the latest highly efficient donor and acceptor materials suitable for semi-transparent OSCs (ST-OSCs).
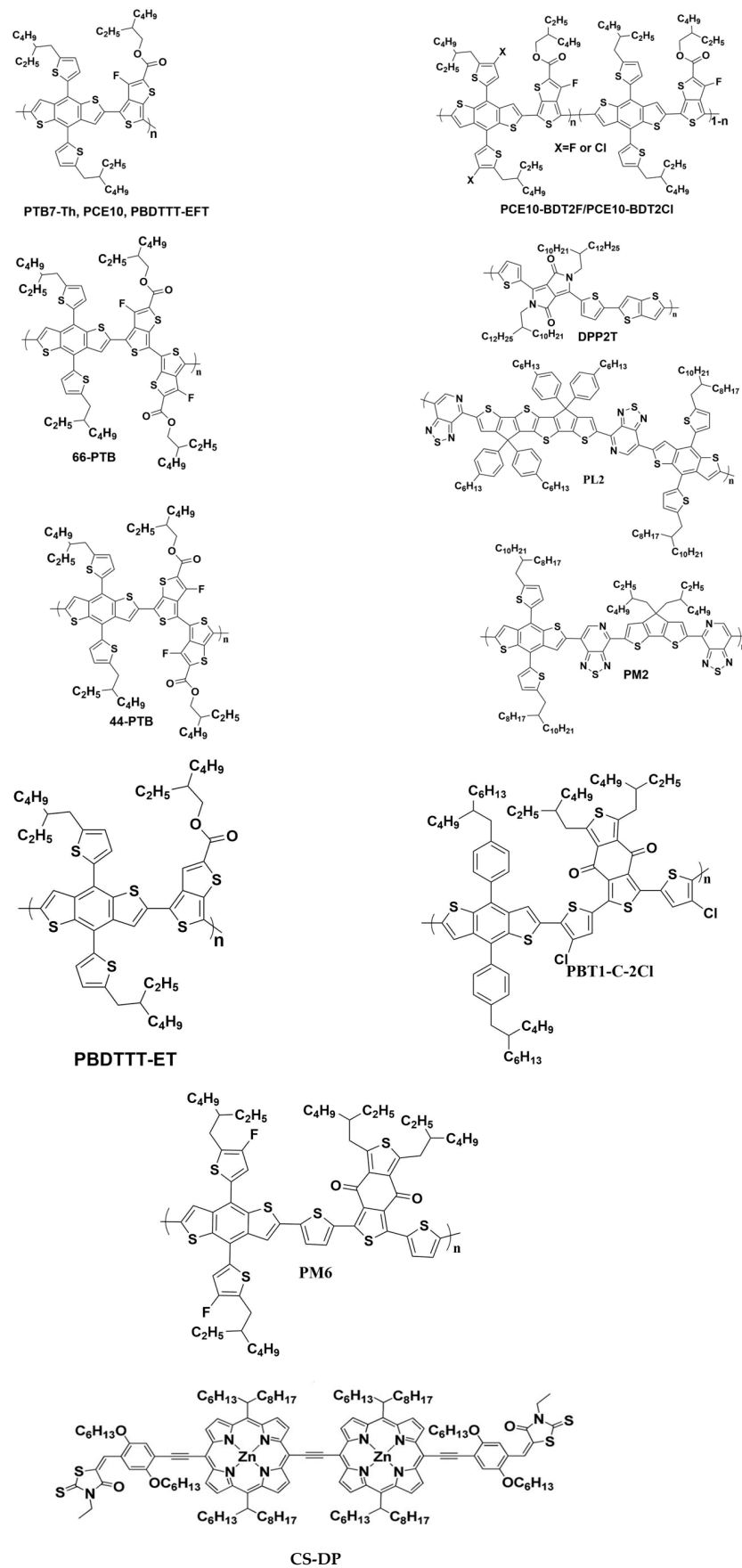
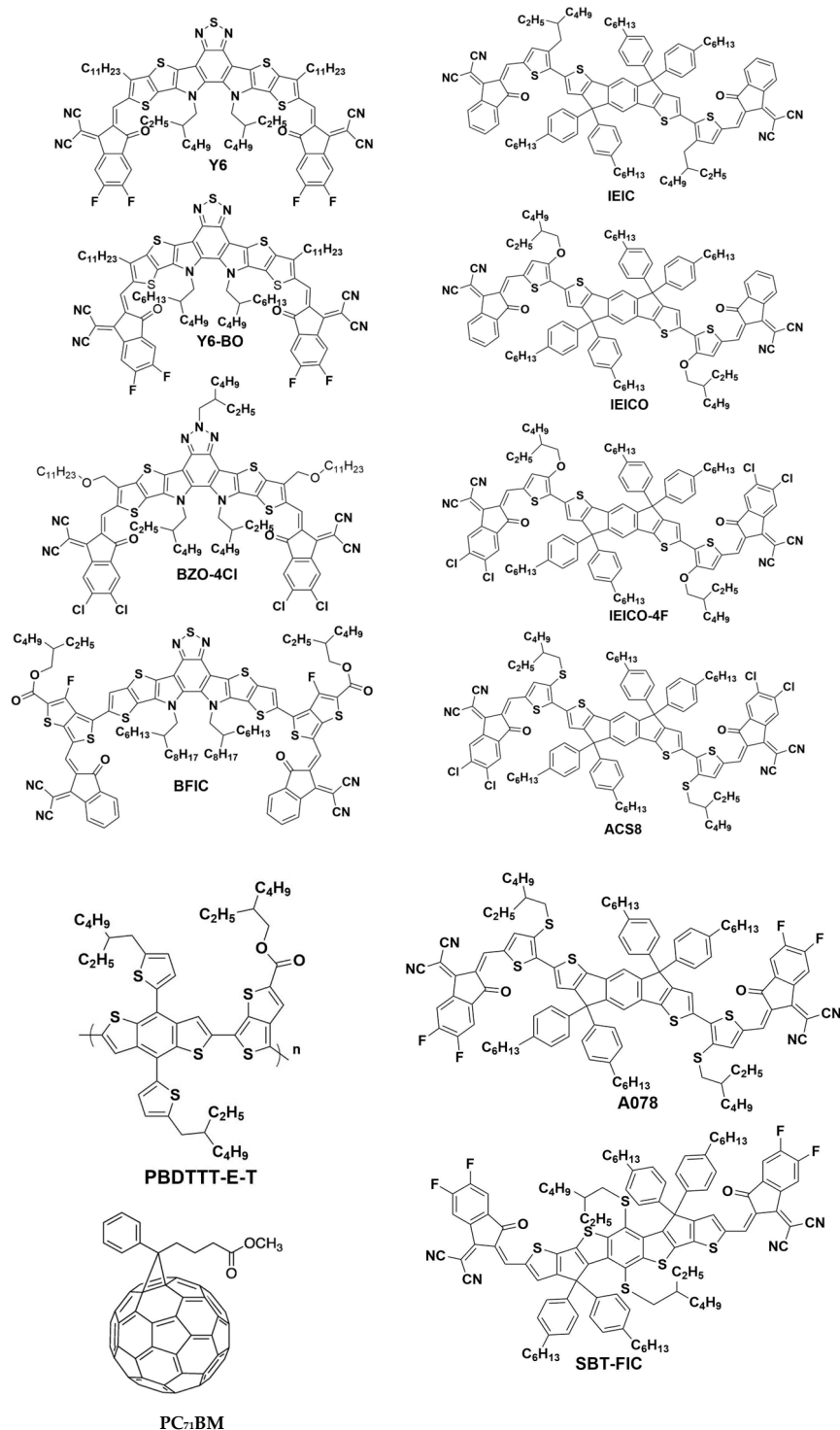**Figure 1.** Molecular structures of novel donor materials.

Figure 2. Molecular structures of novel acceptor materials.

2. Novel Materials for Semi-Transparent OSCs

This section focuses on highly efficient NIR-active materials used to develop semi-transparent OSCs. In exploring high-performing ST-OSCs, the trade-off between PCE and average visible transmittance (AVT) has long been a challenging hurdle. Devices' overall efficiency is defined by Light Utilization Efficiency (LUE), which is the product of PCE and AVT [37].

The recent innovations in ST-OSCs are particularly noteworthy, especially the novel donor materials that absorb more efficiently in the NIR region. To synthesize donor

material useful for ST-OSCs by narrowing the bandgap of the donor polymer, Kini et al. [22] described two primary strategies, as shown in Figure 3a. The first strategy involves the synthesis of polymers using a donor–acceptor (D–A) molecular architecture. This is a unique push–pull molecular architecture featuring alternating electron-rich and electron-deficient units, known as "D" and "A", respectively [38–41]. This configuration results in an efficient intramolecular charge transfer (ICT), effectively narrows the polymer's bandgap, and thus enhances its ability to absorb NIR radiation [39,42,43]. This approach not only reduces the bandgap of polymer donors through the hybridization of HOMO and LUMO between the "D" and "A" components but also facilitates electron delocalization along the polymer backbone, thanks to a strong push–pull effect. The second strategy focuses on stabilizing the structure through quinoidal resonance along the conjugated backbone. This method is effective because quinoidal structures tend to have a lower bandgap compared to aromatic structures. Figure 3b illustrates the chemical structures of some polymer donors used in fullerene-based ST-OSCs, showcasing these approaches.
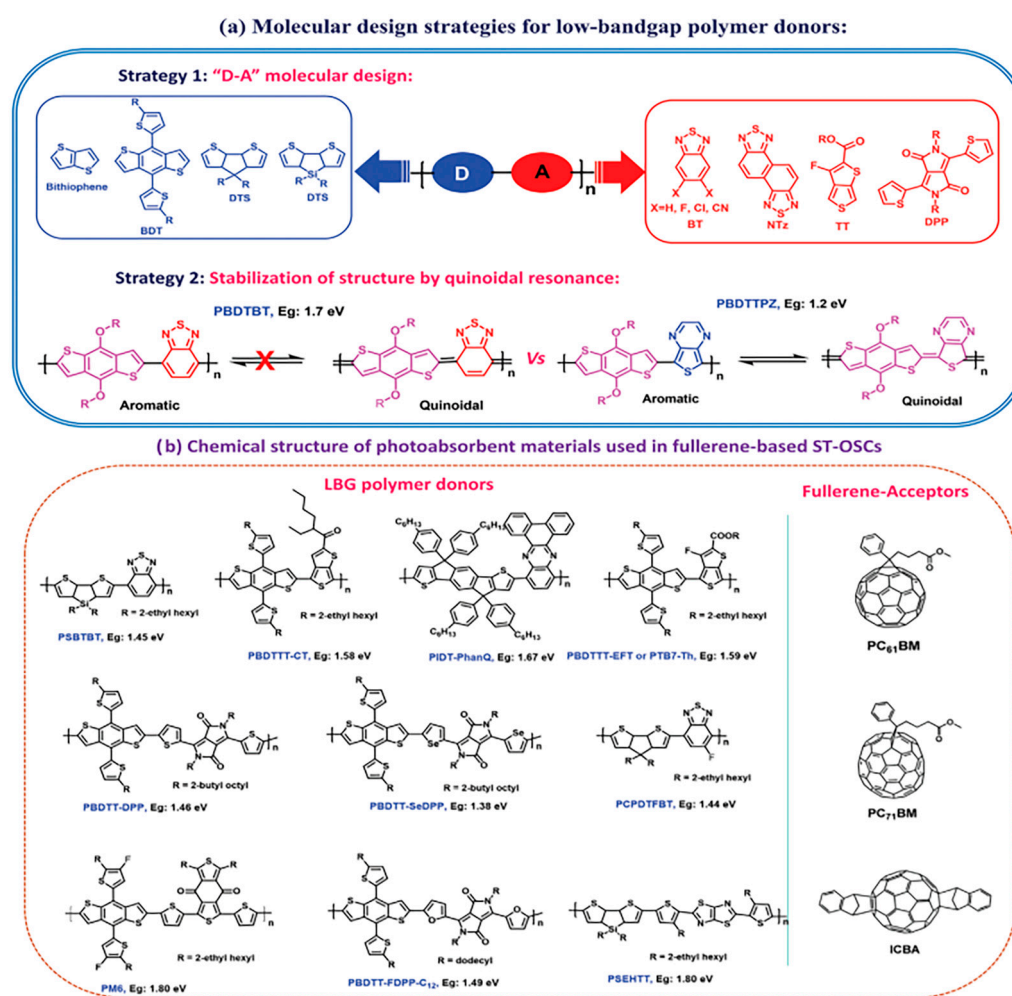

Figure 3. (**a**) Molecular design strategies for synthesizing low-bandgap polymer donors and (**b**) the chemical structure of materials for ST-OSCs. (Republished with permission [22], 2021, John Wiley and Sons).

Over the last few years, a variety of materials have been commonly used as the D units in copolymers for OSC devices. These include benzo [1,2-b:4,5-b′]dithiophene (BDT) [44], carbazole [45], thiophene [46,47], and benzo [1,2-b:4,5-b′]difuran [48,49]. As for the A units, the most frequently employed materials are benzothiadiazole [50–52], benzotriazole [53], and benzodithiophene-4,8-dione (BDD) [54]. Researchers have experimented with several structural modifications to enhance the photovoltaic performance of these copolymers.

Approaches to fine-tuning their properties have included fluorination, chlorination, and side-chain engineering. By strategically deploying this push–pull architecture, researchers are making strides in elevating both the PCE and the LUE, thereby inching closer to a more balanced and efficient semi-transparent photovoltaic system. PTB7-Th, which is commonly utilized in OSCs due to its semi-transparency [55,56], exemplifies this with a D-A backbone comprising benzodithiophene (BDT) and fluorinated thienothiophene (FTT). Unique to PTB7-Th is its "regioregularity", an attribute influenced by the asymmetry in the FTT unit, which in turn significantly impacts both physicochemical properties and device performance [57]. Researchers have experimented with modifying the molecular architecture to a D-A-A configuration to further enhance ICT by incorporating two FTT units. This led to the development of the polymers 44-PTB and 66-PTB. Impressively, 66-PTB exhibited robust NIR absorption between 650 nm and 850 nm, owing to the dual FTT units at the 6-position. In contrast, 44-PTB, having FTT units at the 4-position, manifested absorption profiles akin to those of PTB7-Th. Differences in backbone planarity due to FTT positioning account for this variability. A blend of 66-PTB with a narrow-bandgap acceptor, IEICO-4F, achieved an optimized PCE of 7.84%, despite the absorption of radiation only in the NIR region [44].

In research conducted by Huang et al. [58], a new approach was taken to improve the compatibility of PTB7-Th (also called PCE10) with Y6, two materials commonly used in OSCs. By introducing a third type of unit into the PTB7-Th matrix, specifically a BDT unit that was modified by a fluorine or chlorine group, two new series of terpolymer donors were created: PCE10-BDT2F and PCE10-BDT2Cl. Notably, the solar cell device made with PCE10-BDT2F-0.8 and Y6 achieved an impressive PCE of 13.80%. This represents a nearly 40% improvement over devices made with the original PCE10 and Y6 combination. The terpolymer design strategy can effectively be used to tailor the properties of the polymer donor, achieving a significantly better performance.

Chen et al. [27] synthesized a unique dimeric porphyrin-cored small molecule, CS-DP, featuring an A–π2–D–π1–D–π2–A architecture. This molecule is distinguished by its narrow bandgap (Eg) of 1.22 eV, allowing it to have an extended absorption spectrum in the 700–1000 nm range. When coupled with $PC_{71}BM$ as an acceptor in Bulk Heterojunction (BHJ) OSCs, the deeper energy levels of the molecule's Highest Occupied Molecular Orbital (HOMO) and Lowest Unoccupied Molecular Orbital (LUMO) contribute to achieving an impressive PCE of 8.29% [27]. In a separate study, Lee et al. developed OSCs based on DPP2T:IEICO-4F that are efficient at converting NIR light into electricity with a PCE of 9.13% while remaining transparent in the visible spectrum, making them ideal for applications where visible-light transparency is desired, such as in transparent windows that can also generate power [59].

Xie et al. [60] explored using a fibril network strategy to achieve both a high AVT and PCE in semi-transparent OSCs. Utilizing wide-bandgap (WBG) PBT1-C-2Cl and Y6 as their electron donor and electron acceptor devices, respectively, they discovered that PBT1-C-2Cl possesses a unique property of self-assembling into fibrillar nanostructures. Adding even a small quantity of PBT1-C-2Cl to the blend resulted in a dramatic increase in hole mobility (μh) by creating charge pathways. This, in turn, also led to an improvement in optoelectronic properties [60].

Hu et al. [61] were pioneers in fabricating semi-transparent OSCs that utilized Y6 as an electron acceptor and PM6 as an electron donor. This blend achieved an exceptional AVT of 50.5% at a thickness of 100 nm and achieved a PCE of 14.2% [61].

Yoon et al. [62] advanced the field by developing a new polymer donor with a cyclopentadithiophene (CPDT) core. This polymer exhibits powerful absorption in the near-infrared (NIR) spectrum without compromising visibility. The deep energy levels of its HOMO also align well with low-bandgap NFAj. Consequently, they engineered an OSC achieving a notable PCE of 9.91% and an AVT of 40.4%, leading to a high LUE of 4% for the PL2 polymer donor with Y6 and $PC_{61}BM$ as acceptors. A PTB7-Th-based system with NFAs demonstrated an LUE of around 3% in contrast to PL2 blends, which achieved a higher

LUE. PL2, with its lower HOMO levels compared to PTB7-Th, offers better compatibility with NFAs [62]. Jiang et al. [63] developed an OSC using a PM2:Y6-BO system with a PCE of over 11%. When compared with PM6-based systems, the PCE of the PM6 system is higher than that of the PM2-based system. However, the AVT of the PM2-based system (an AVT of 32.7%) is higher than that of the PM6-based system (an AVT of 20.9%). This research also identified challenges with the PM2-based semi-transparent OSCs, as they grappled with charge recombination and energy loss issues, indicating avenues for further refinement and optimization in this promising OSC system.

In recent times, the focus of OPV research has also increasingly moved toward NFAs, which offer several advantages over traditional fullerene-based materials. NFAs are typically structured using architectures like "A–D–A", "A-DA′D-A", or "A–(π-spacer)–D–(π-spacer)–A", where a core-electron-donating fused-ring heterocycle, marked as "D" and "DA′D", is linked to terminal "A" groups through either vinyl linkages or π-spacer units [64]. By tweaking these core-donating units, side groups, π-spacers, and terminal acceptor units through chemical modification, it becomes possible to selectively optimize their optoelectronic characteristics, molecular arrangement, charge mobility, and overall PCEs. One notable example of this process is the development of Y-series NFAs, beginning with the Y1 molecule. This innovation in the field of organic photovoltaics has been a pivotal factor in the increased PCEs observed in Y-NFA-based OSCs. Building upon this, Yang [65] outlined strategies to further improve the efficiency of Y-NFA, as illustrated in Figure 4. These modifications may involve integrating sp^2-hybridized heteroatoms and inserting π-bridges to improve the π-conjugation system. Optimizing the side chains in different positions with a variety of chemical structures is another strategy, which aims to enhance the active layer's morphology. Furthermore, the central "A" unit and end group can also be modified. With the high performance already achieved in OPVs utilizing Y-NFAs, such structural adjustments to the Y1 molecule are poised to lead to the creation of new, high-performing acceptor molecules. This approach underscores the dynamic potential of NFAs in elevating the performance of OSCs [65].
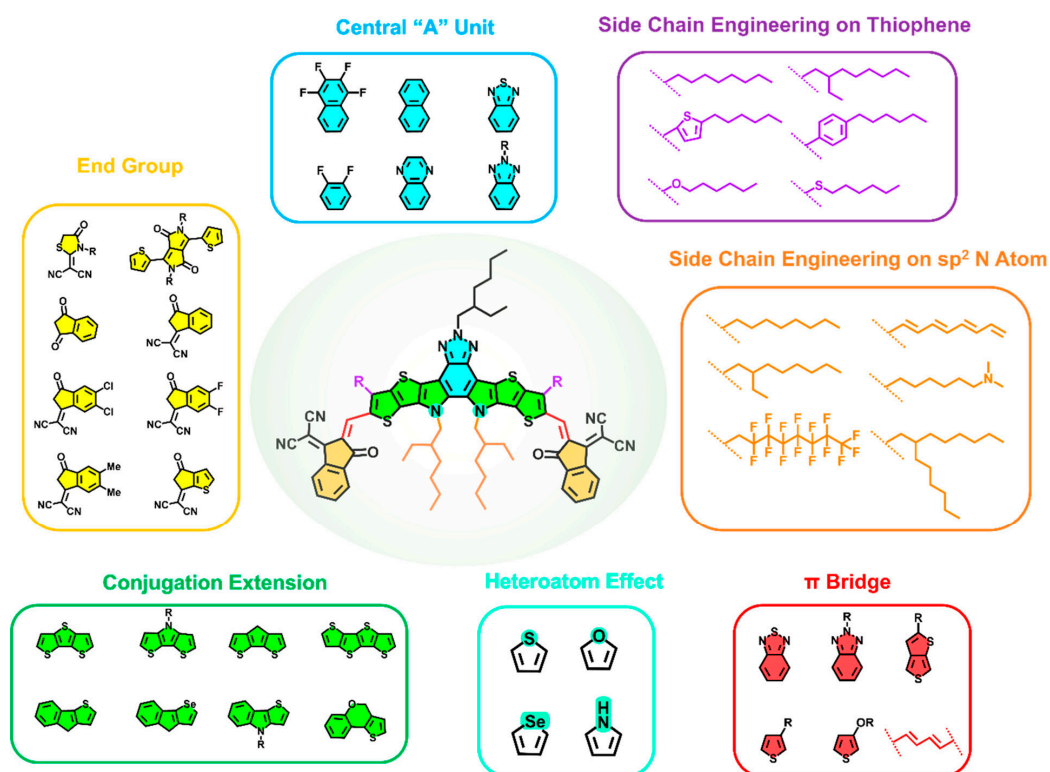

Figure 4. Strategies for exploring innovative Y-Series non-fullerene acceptors [65].

A common strategy to enhance NIR absorption in NFAs is to include terminal "A" units featuring varied functional groups, which increases the electron-withdrawing effect. Recent research highlights that these terminal "A" units impact photophysical characteristics and the energy bandgap (Eg) and affect molecular orientation and overall morphology due to non-covalent interactions [22]. The chemical structures of recently used highly efficient acceptor materials for ST-OSCs are shown in Figure 2.

Incorporating a π-spacer into the "A–D–A" molecular architecture to create "A–π–D–π–A"-type NFAs is a widely used strategy for extending π-conjugation and fine-tuning photochemical characteristics and solubility. Introducing heteroatoms or appending suitable soluble alkyl chains to these units often achieves this. These π-spacers have added benefits, including increased charge transport and solid-state packing through non-covalent conformational locking, due to enhanced coplanarity. They also have lower synthetic complexity in comparison to highly conjugated fused-ring cores. Frequently used electron-rich units for π-spacers include thiophene, selenophene, and benzene derivatives, while electron-deficient units often consist of benzothiadiazole (BT) or ester-substituted thiazoles [22].

Yao et al. [66] presented a modified material known as IEICO, in which they replaced the alkyl-substituted thiophene spacer in IEIC with an alkoxy-thiophene unit. This change led to a significant increase in coplanarity and a longer π-conjugation due to non-covalent S···O interactions, resulting in strong NIR absorption with an absorption edge at approximately 925 nm (Eg = 1.34 eV). The modification also led to slightly higher HOMO levels and comparable LUMO values when compared with IEIC. By leveraging these unique properties of IEICO with the complementary absorbing material PBDTTT-ET, Xie et al. [60] developed semi-transparent OSCs that achieved a PCE of 9%, a high Jsc of 16.3 mA cm^{-2}, and an AVT of 17% through efficient NIR photon harvesting. These devices also demonstrated PCEs above 7%, along with an AVT and Incident Photon-to-Current Efficiency (IPCE) of 26.2% and 80.6%, respectively [60]. In a subsequent study, researchers enhanced the IEICO structure by replacing the DIC end groups with more potent electron-withdrawing 2F-DIC units, resulting in a new acceptor unit called IEICO-4F. This modification led to an exceptionally narrow energy bandgap (Eg) of 1.24 eV, thanks to the combined effects of an extended π-conjugation length and a stronger ICT effect induced by the 2F-DIC units. This resulted in an absorption onset situated at 1000 nm in the NIR region, which is 0.1 eV lower than the original IEICO, optimizing the material for effective NIR radiation harvesting. To test the capabilities of this new material, Hu et al. [67] formulated semi-transparent OSC devices using a blend of IEICO-4F and PTB7-Th (in a 1.2:1.5 weight ratio). The devices achieved a remarkable Jsc of 20.59 mA cm^{-2} and a PCE of approximately 9.5%, along with an AVT of 23.7%, J_{sc} of 20.59 mA cm^{-2}, V_{oc} of 0.718 V, and FF of 9.48. They strategically reduced the content of WBG-PD in the active layer to achieve these results. Pure PTB7-Th exhibits its main absorption peak at 700 nm, which is complementary to IEICO-4F's NIR absorption. By reducing the PTB7-Th content in the PTB7-Th:IEICO-4F blend, the researchers successfully minimized photon harvesting in the visible spectrum while enhancing it in the NIR spectrum. This adjustment enabled the researchers to achieve an optimal balance between PCE and AVT [67,68].

Chen et al. [69] modified the IEICO-4F structure by substituting the alkoxy-thiophene linker with an alkylthio-thiophene unit, creating a new material known as ACS8. The solid-state aggregation of alkylthio-alkyl chains in ACS8 resulted in both NIR absorption capabilities and an energy gap (Eg) of 1.3 eV, which is 0.06 eV higher than that of its predecessor, IEICO-4F, having a bandgap of 1.24 eV. Moreover, ACS8 demonstrates an electron mobility of 2.65×10^{-4} cm^2/Vs, outperforming IEICO-4F, which shows a mobility of only 1.14×10^{-4} cm^2/Vs. This new molecule also exhibited impressive PCE values ranging from 9.4% to 11.1%, alongside a varying AVT between 43.2% and 28.6% depending upon the thickness of the silver (Ag) layer [69].

To further understand the influence of alkylthio-alkyl side chains, the researchers compared the absorption spectrum of A078, which has a partially fused core, to that of its fully fused analog, SBT-FIC. Intriguingly, A078 demonstrated a substantial bathochromic shift

and more compact molecular packing than SBT-FIC. This finding highlights the importance of non-covalent S···S interactions in facilitating the planarization and rigidification of the π-conjugated structure, which in turn narrows the energy gap. Taking advantage of ACS8's compatibility with semi-transparent OSCs due to its transparency in the visible spectrum, the team achieved a PCE of 11.0% and a 25% AVT [70].

In a study conducted by Zhang et al. [71], a novel NIR material called the BFIC acceptor was developed. Utilizing an A−π−D−π−A molecular architecture, the material incorporates FTT as a π-bridge. This dual-function inclusion extends the molecular conjugation and stabilizes its resonance structure. Furthermore, the weak electron-withdrawing capacity of FTT enhances the ICT, effectively narrowing BFIC's bandgap. The BFIC material exhibits a wide and intense NIR absorption spectrum that ranges from 700 to 1050 nm. This is further enhanced by the non-covalent interactions triggered by the fluorine atom in FTT, which optimizes molecular packing in the solid state. BFIC is highly compatible with the donor polymer PTB7-Th due to well-aligned energy levels. Regarding the thin-film absorption of BFIC, there is a shift toward longer wavelengths, peaking at 925 nm. This behavior indicates strong intermolecular packing and is a testament to the efficacy of its molecular architecture. Importantly, BFIC features an ultra-narrow E_g of 1.18 eV, which was confirmed by its absorption onset extending to 1050 nm on the optical spectrum. These properties contribute to the notable PCE of 10.38% of OSCs that are constructed using PTB7-Th and BFIC. In a semi-transparent OSC variant, a PCE of 6.15% was obtained, along with an AVT of 38.79%. This study also revealed that FTT incorporation is beneficial for the improvement of PCE [71].

In a research study conducted by Xu et al. [72], a novel A-DA'D-A acceptor named BZO-4Cl was developed. This material boasts an exceptionally low optical bandgap of 1.26 eV and an absorption that is shifted by approximately 60 nm toward longer wavelengths when compared to the material Y6. When examining the films, PTB7-Th combined with BZO-4Cl demonstrated good π–π stacking. Additionally, a pronounced backbone peak was observed, likely arising from an extended backbone ordering. This feature is key to augmenting the Jsc and fill factor (FF) of OSCs. Further, the blended film of PTB7-Th and BZO-4Cl exhibited an optimal morphology, which led to several benefits: increased charge generation and transport and decreased charge recombination. A significant factor behind the enhanced efficiency of the PTB7-Th: BZO-4Cl device is its minimized energy loss, which is attributed primarily to a drop in radiative recombination loss when compared to the Y6-integrated device. As a testament to its efficiency, the non-transparent variant of the PTB7-Th: the BZO-4Cl device achieved an impressive PCE of 14.12%. After further refinement for semi-transparency, the device achieved a PCE of 9.33%, an AVT of 43.08%, an LUE of 4.02%, and remarkable color rendering, with a color rendering index (CRI) exceeding 90% [72].

Recently, there has been significant interest in non-fused-ring Small-Molecule Acceptors (SMAs) because of their straightforward synthesis, diverse structures, and adjustable morphology. These SMAs have achieved an impressive PCE exceeding 15% due to their molecular designs, which utilize conformational lock strategies. These "locks" are often realized through non-covalent bonds, which help stabilize the molecule's structure. For instance, past research identified two non-covalent interactions, S···O and C–H···O, which keep the planar structure of conjugated polymers stable, thereby enhancing carrier mobility. Other interactions, like C–H···F, S···N, and S···Cl, have also been employed in crafting SMAs, resulting in improved PCEs between 13 and 15%. Specifically, Zhu et al. [73] designed two asymmetric dual-donor SMAs named IOEH-N2F and IOEH-4F. While both shared a common central unit, they had different terminals. The IOEH-N2F variant, with its specific terminal structure, displayed a broader planar structure, better crystallinity, and enhanced NIR absorption compared to IOEH-4F. As a result, devices using IOEH-N2F achieved a remarkable PCE of 14.25%, an 18% improvement over those utilizing IOEH-4F. These findings underscore the potential of tweaking electron-withdrawing terminals in asymmetric acceptors to enhance both performance and cost-efficiency in OSCs [73].

Innovative molecular architecture designs are driving remarkable advances in the field of organic semiconductors, paving the way for new levels of efficiency and versatility. While challenges persist, the architecture of these materials holds immense promise for applications such as BIPV. Table 1 summarizes the optoelectronic properties of novel materials.

Table 1. Optoelectronic properties of novel materials.

Donor	$^{Donor}E_g^{Opt.}$ (eV)	E_{LUMO}/E_{HOMO} (Donor)	Acceptor	$^{Acceptor}E_g^{Opt.}$ (eV)	E_{LUMO}/E_{HOMO} (Acceptor)	V_{OC} (V)	J_{SC} (mA cm^{-2})	FF (%)	PCE (%)	AVT (%)	Ref.
PM6	1.81	3.50/5.56	Y6	1.33	4.10/5.65	0.83	25.3	76.1	15.7	-	[31]
PCE10-BDT2F	1.59	3.82/5.42	Y6	-	4.10/5.66	0.751	20.73	69.74	10.85	41.08	[58]
CS-DP	1.26	3.74/4.96	PC$_{71}$BM	-	-	0.796	15.19	70.0	8.29	-	[27]
PL2	1.51	3.98/5.49	Y6:PC$_{61}$BM	-	-	0.69	24.07	59.74	9.91	40.4	[62]
PM2	1.41	3.89/5.30	Y6-BO	1.30	4.38/5.68	0.71	16.2	68.9	7.9	32.7	[63]
PM6	1.84	3.70/5.54	Y6-BO	1.30	4.38/5.68	0.81	19.1	73.5	11.4	20.9	[63]
PM6	[31]	-	Y6	1.33	4.10/5.65	0.855	25.39	72.93	15.83	50.5	[61]
PBT1-C-2Cl	1.85	-	Y6	1.33	-	0.83	15.71	67.7	9.1	40.1	[60]
PBDTTT-E-T	-	-	IEIC	1.50	-	0.90	11.7	47	4.9	-	[66]
PBDTTT-E-T	-	-	IEICO	1.34	3.95/5.32	0.82	17.7	58	8.4	-	[66]
PTB7-Th	-	-	IEICO-4F	-	-	0.718	20.59	64.0	9.48	23.7	[67]
PTB7-Th	-	3.33/5.30	ACS8	1.30	4.05/5.54	0.74	19.9	63.8	9.4	43.2	[69]
PTB7-Th	-	-	A078	1.40	4.06/5.58	0.75	21.2	73	11.3	47.8	[70]
PTB7-Th	-	-	SBT-FIC	1.65	4.15/5.81	0.71	18.7	65	8.2	-	[70]
PTB7-Th	-	3.64//5.24	BFIC	1.18	4.00/5.26	0.66	13.82	65.4	6.15	38.79	[71]
PTB7-Th	-	3.04/5.34	BZO-4Cl	1.26	3.97/5.71	0.708	19.73	66.69	9.33	43.08	[72]
PM6	-	3.64/5.45	IOEH-N2F	1.34	3.98/5.44	0.846	22.63	74.41	14.25	-	[73]
PM6	-	3.64/5.45	IOEH-4F	1.38	3.99/5.46	0.874	17.81	75.55	11.77	-	[73]

3. Discussion

This discussion focuses on the critical strategies for developing materials for semi-transparent organic solar cells (OSCs). A pivotal approach to enhancing the optoelectronic properties of these materials lies in molecular tailoring. This process involves various modifications, such as altering alkyl chains, incorporating electron-donating/withdrawing groups, and utilizing donor–acceptor configurations in copolymerization. These modifications are essential for optimizing the photovoltaic performance of OSCs.

The advancement of ST-OSCs hinges on the innovative molecular engineering of polymer donors, particularly in the context of NIR absorption. By manipulating molecular structures and incorporating specific design strategies, significant improvements in device performance can be achieved. For example, by employing a unique push–pull molecular architecture, which alternates between electron-rich (donor or "D") and electron-deficient (acceptor or "A") units, an efficient intramolecular charge transfer is achieved. This not only narrows the polymer's bandgap but also augments its NIR absorption capabilities. For instance, the asymmetric FTT unit in polymers like 44-PTB and 66-PTB, with different connection sites, leads to variations in polymer structure and properties. Notably, 66-PTB displays a more planar backbone than 44-PTB, extending its conjugation length and enhancing its ICT effect, which results in a greater red shift in NIR absorption. A terpolymer design strategy, adjusting the characteristics of the PCE10 polymer donor, has also been adopted in the literature. The inclusion of fluorine (F) or chlorine (Cl) atoms, which are known for their strong electron affinity, effectively lowers the energy levels and boosts the extinction coefficient of the resulting terpolymers. For example, incorporating structurally similar BDT-2F or BDT-2Cl can improve a face-on orientation and improve the compatibility with Y6, enhancing charge transport.

Furthermore, the progression from IEIC to IEICO, and then to IEICO-4F, exemplifies how specific molecular modifications can improve critical parameters like the short-circuit current (JSC) and fill factor (FF). The transition to IEICO-4F, in particular, demonstrates a notable efficiency improvement when paired with a PTB7-TH donor, achieving an average visible transmittance (AVT) of 23.7%. This highlights the importance of fine-tuning acceptor materials. Further advances in IEIC derivatives led to the development of ACS8 and A078 acceptors. These variants showed even higher AVTs of 43.2% and 47.8%, respectively, when combined with the PTB7-Th donor. Such improvements underscore the significance of continuous innovation in acceptor materials for enhancing light transmittance and efficiency.

The choice of donor–acceptor combinations is also crucial in determining the overall device performance. For example, pairing PM6 as a donor with Y6 as an acceptor, under controlled morphological conditions, yielded a high power conversion efficiency (PCE) of 15.83% and an AVT of 50.5% [61]. This outperforms other combinations like PCE10-BDT2F, PBT1-C-2Cl, and PL2 with the Y6 acceptor. It is also possible that slight changes in the molecular structure of a material may optimize the overall performance. For example, the IOEH-N2F acceptor variant, with its distinct terminal structure, offers a broader planar structure, improved crystallinity, and enhanced near-infrared (NIR) absorption compared to its counterpart, the IOEH-4F acceptor, even with the same donor, such as PM6.

These examples illustrate that novel materials can be strategically selected for specific applications, balancing between PCE and AVT. Such strategic molecular tailoring and the careful selection of donor–acceptor combinations are key in advancing the field of semi-transparent OSCs, pushing the boundaries of their efficiency and applicability in real-world scenarios. However, a significant limitation in the deployment of highly efficient materials for semi-transparent OSCs is the instability of these materials, which presents a major barrier to their commercialization. This instability often results from the molecular aggregation of small molecules within the thin film. Over time, this aggregation can lead to morphological changes that detrimentally affect both the performance and longevity of the OSCs. The challenge lies in maintaining stability under various environmental conditions, such as exposure to heat, light, and moisture, which is a critical issue that must be addressed to ensure the practical viability of these solar cells.

Ultimately, overcoming the challenge of material instability in semi-transparent OSCs is crucial for unlocking their full commercial potential. Addressing this limitation will enable more reliable integration of semi-transparent OSCs into building designs. Doing so contributes significantly to sustainable energy solutions and represents a leap forward in architectural innovation.

4. Conclusions and Outlook

This section provides a conclusion and looks ahead to future prospects. The transparency characteristic of semiconductor materials provides opportunities for specialized applications, such as semi-transparent OSCs. Such applications prominently include Building-Integrated Photovoltaics (BIPV), which can be seamlessly integrated into windows, rooftops, and façades, generating electricity and contributing to the aesthetics of the built environment.

One effective way to improve the performance of these devices is by customizing efficient materials at the molecular level. Among the numerous methods available for this molecular tailoring, the development of copolymers with a push–pull architecture stands out. This strategy relies on donor–acceptor configurations, providing many possible combinations. Furthermore, by introducing electron-donating and -withdrawing groups, one can fine-tune the HOMO/LUMO energy levels and optimize the bandgap of the material, thus driving better performance.

Moreover, the focus on designing active materials in the near-infrared spectrum offers a unique advantage for semi-transparent OSCs. Harnessing the potential of near-infrared can further optimize efficiency and transparency as well, making them even more beneficial for building applications.

The implications of such advances are profound. With buildings contributing significantly to global warming, the incorporation of semi-transparent OSCs in their design can play a pivotal role in mitigating the associated environmental impact. The market potential for these applications is substantial.

However, a significant challenge lies ahead: ensuring the long-term stability of these devices.

As with any technology intended for real-world applications, durability becomes a paramount concern, especially under harsh environmental conditions. Therefore, as we chart the course for the future of the semi-transparent OSCs, research must pivot toward ad-

dressing and overcoming these stability challenges to truly unlock their commercial potential and realize their environmental promise. Embracing the potential of semi-transparent OSCs could redefine our architectural landscape, bridging the gap between aesthetics, functionality, and environmental responsibility.

Although many OSCs have shown impressive PCEs, the intricate methods required for synthesizing these high-performing materials add complexity and cost. Additionally, the question of long-term stability remains unresolved. Some OSC compositions have shown promising resilience, maintaining up to 80% of their initial PCE for projected periods of over two decades [74]. However, these stable configurations are not necessarily the ones setting PCE records. Notably, leading-edge materials such as PM6:Y6 and their analogs have not yet demonstrated this level of durability. Complicating the matter further, OSCs are subjected to thermal cycling under real-world weather conditions, a factor known to compromise the morphology of the active layer and diminish efficiency over time. For OSC technology to successfully transition from the laboratory to the marketplace, two critical issues must be addressed: enhancing device longevity without losing PCE and simplifying the synthesis of advanced materials [75,76]. These missions can be achieved by conducting further research for the improvement in the stability of OSCs. Now, the challenge is to overcome the stability issue of efficient materials without compromising on their efficiencies and to simplify synthetic procedures to reduce the cost.

The literature indicates various solutions to OSC instability, which is primarily caused by material degradation under thermal, chemical, and light exposure. A significant concern in Small-Molecule Acceptor (SMA)-based OSCs is thermal degradation due to microphase separation or molecular aggregation between the donor and acceptor in films. This separation decreases carrier mobility and charge generation due to loss of initial morphology, thereby reducing device performance, shelf-life, and thermal stability. One effective strategy used to enhance thermal stability in OSCs is the crosslinking of donor and/or acceptor materials. This approach helps maintain the thin-film morphology in OSCs devices. Additionally, implementing robust encapsulation and designing materials with steric groups, isomeric sites, and photoactive sites are other methods of mitigating OSC instability. These approaches are crucial for advancing OSC technology toward practical and commercial applications [77,78].

References

1. Sustainable Development Goals. Available online: https://sdgs.un.org/goals (accessed on 27 September 2023).
2. Scott, D.; Hall, C.M.; Gössling, S. Global Tourism Vulnerability to Climate Change. *Ann. Tour. Res.* **2019**, *77*, 49–61. [CrossRef]
3. Ortiz-Bobea, A.; Ault, T.R.; Carrillo, C.M.; Chambers, R.G.; Lobell, D.B. Anthropogenic Climate Change Has Slowed Global Agricultural Productivity Growth. *Nat. Clim. Change* **2021**, *11*, 306–312. [CrossRef]
4. Cavicchioli, R.; Ripple, W.J.; Timmis, K.N.; Azam, F.; Bakken, L.R.; Baylis, M.; Behrenfeld, M.J.; Boetius, A.; Boyd, P.W.; Classen, A.T.; et al. Scientists' Warning to Humanity: Microorganisms and Climate Change. *Nat. Rev. Microbiol.* **2019**, *17*, 569–586. [CrossRef]
5. Gong, J.; Li, C.; Wasielewski, M.R. Advances in Solar Energy Conversion. *Chem. Soc. Rev.* **2019**, *48*, 1862–1864. [CrossRef]
6. Timilsina, G.R.; Kurdgelashvili, L.; Narbel, P.A. Solar Energy: Markets, Economics and Policies. *Renew. Sustain. Energy Rev.* **2012**, *16*, 449–465. [CrossRef]
7. Yu, H.; Wang, J.; Zhou, Q.; Qin, J.; Wang, Y.; Lu, X.; Cheng, P. Semi-Transparent Organic Photovoltaics. *Chem. Soc. Rev.* **2023**, *52*, 4132–4148. [CrossRef]

8. Yoshikawa, K.; Kawasaki, H.; Yoshida, W.; Irie, T.; Konishi, K.; Nakano, K.; Uto, T.; Adachi, D.; Kanematsu, M.; Uzu, H.; et al. Silicon Heterojunction Solar Cell with Interdigitated Back Contacts for a Photoconversion Efficiency over 26%. *Nat. Energy* **2017**, *2*, 17032. [CrossRef]

9. Green, M.; Dunlop, E.; Hohl-Ebinger, J.; Yoshita, M.; Kopidakis, N.; Hao, X. Solar Cell Efficiency Tables (Version 57). *Prog. Photovolt. Res. Appl.* **2021**, *29*, 3–15. [CrossRef]

10. Stuckelberger, M.; Biron, R.; Wyrsch, N.; Haug, F.J.; Ballif, C. Review: Progress in Solar Cells from Hydrogenated Amorphous Silicon. *Renew. Sustain. Energy Rev.* **2017**, *76*, 1497–1523. [CrossRef]

11. Green, M.A.; Dunlop, E.D.; Siefer, G.; Yoshita, M.; Kopidakis, N.; Bothe, K.; Hao, X. Solar Cell Efficiency Tables (Version 61). *Prog. Photovolt. Res. Appl.* **2023**, *31*, 3–16. [CrossRef]

12. Mallick, R.; Li, X.; Reich, C.; Shan, X.; Zhang, W.; Nagle, T.; Bok, L.; Bicakci, E.; Rosenblatt, N.; Modi, D.; et al. Arsenic-Doped CdSeTe Solar Cells Achieve World Record 22.3% Efficiency. *IEEE J. Photovolt.* **2023**, *13*, 510–515. [CrossRef]

13. Szabó, G.; Park, N.-G.; De Angelis, F.; Kamat, P.V. Are Perovskite Solar Cells Reaching the Efficiency and Voltage Limits? *ACS Energy Lett.* **2023**, *8*, 3829–3831. [CrossRef]

14. Wang, J.; Zheng, Z.; Bi, P.; Chen, Z.; Wang, Y.; Liu, X.; Zhang, S.; Hao, X.; Zhang, M.; Li, Y.; et al. Tandem Organic Solar Cells with 20.6% Efficiency Enabled by Reduced Voltage Losses. *Natl. Sci. Rev.* **2023**, *10*, nwad085. [CrossRef] [PubMed]

15. Mohamed El Amine, B.; Zhou, Y.; Li, H.; Wang, Q.; Xi, J.; Zhao, C. Latest Updates of Single-Junction Organic Solar Cells up to 20% Efficiency. *Energies* **2023**, *16*, 3895. [CrossRef]

16. He, W.; Li, H.; Ma, R.; Yan, X.; Yu, H.; Hu, Y.; Hu, D.; Qin, J.; Cui, N.; Wang, J.; et al. In Situ Self-Assembly of Trichlorobenzoic Acid Enabling Organic Photovoltaics with Approaching 19% Efficiency. *Adv. Funct. Mater.* **2023**. *early view*. [CrossRef]

17. Ji, J.M.; Zhou, H.; Eom, Y.K.; Kim, C.H.; Kim, H.K. 14.2% Efficiency Dye-Sensitized Solar Cells by Co-Sensitizing Novel Thieno[3,2-b]Indole-Based Organic Dyes with a Promising Porphyrin Sensitizer. *Adv. Energy Mater.* **2020**, *10*, 2000124. [CrossRef]

18. Chrispim, M.C. Resource Recovery from Wastewater Treatment: Challenges, Opportunities and Guidance for Planning and Implementation. Ph.D. Thesis, University of Sao Paulo, Sao Paulo, Brazil, 2021.

19. Rabaia, M.K.H.; Abdelkareem, M.A.; Sayed, E.T.; Elsaid, K.; Chae, K.J.; Wilberforce, T.; Olabi, A.G. Environmental Impacts of Solar Energy Systems: A Review. *Sci. Total Environ.* **2021**, *754*, 141989. [CrossRef]

20. Li, Y.; Huang, X.; Sheriff, H.K.M.; Forrest, S.R. Semitransparent Organic Photovoltaics for Building-Integrated Photovoltaic Applications. *Nat. Rev. Mater.* **2023**, *8*, 186–201. [CrossRef]

21. Wang, W.; Brown, M.K. Photosensitized [4+2]- and [2+2]-Cycloaddition Reactions of *N*-Sulfonylimines. *Angew. Chem. Int. Ed.* **2023**, *62*, e202305622. [CrossRef]

22. Kini, G.P.; Jeon, S.J.; Moon, D.K. Latest Progress on Photoabsorbent Materials for Multifunctional Semitransparent Organic Solar Cells. *Adv. Funct. Mater.* **2021**, *31*, 2007931. [CrossRef]

23. Meng, D.; Zheng, R.; Zhao, Y.; Zhang, E.; Dou, L.; Yang, Y. Near-Infrared Materials: The Turning Point of Organic Photovoltaics. *Adv. Mater.* **2022**, *34*, 2107330. [CrossRef] [PubMed]

24. Chen, D.; Nakahara, A.; Wei, D.; Nordlund, D.; Russell, T.P. P3HT/PCBM Bulk Heterojunction Organic Photovoltaics: Correlating Efficiency and Morphology. *Nano Lett.* **2011**, *11*, 561–567. [CrossRef] [PubMed]

25. Kim, J.Y. Determining the Effect of Different Heat Treatments on the Electrical and Morphological Characteristics of Polymer Solar Cells. *Energies* **2019**, *12*, 4678. [CrossRef]

26. Lim, D.H.; Ha, J.W.; Choi, H.; Yoon, S.C.; Lee, B.R.; Ko, S.J. Recent Progress of Ultra-Narrow-Bandgap Polymer Donors for NIR-Absorbing Organic Solar Cells. *Nanoscale Adv.* **2021**, *3*, 4306–4320. [CrossRef] [PubMed]

27. Chen, S.; Yan, L.; Xiao, L.; Gao, K.; Tang, W.; Wang, C.; Zhu, C.; Wang, X.; Liu, F.; Peng, X.; et al. A Visible-near-Infrared Absorbing A-Π2-D-Π1-D-Π2-A Type Dimeric-Porphyrin Donor for High-Performance Organic Solar Cells. *J. Mater. Chem. A Mater.* **2017**, *5*, 25460–25468. [CrossRef]

28. Xiao, L.; Li, Z.; Hu, Q.; Liu, Y.; Zhong, W.; Mei, X.; Russell, T.P.; Liu, Y.; Min, Y.; Peng, X.; et al. Improving the Efficiencies of Small Molecule Solar Cells by Solvent Vapor Annealing to Enhance J-Aggregation. *J. Mater. Chem. C Mater.* **2019**, *7*, 9618–9624. [CrossRef]

29. Ashraf, R.S.; Meager, I.; Nikolka, M.; Kirkus, M.; Planells, M.; Schroeder, B.C.; Holliday, S.; Hurhangee, M.; Nielsen, C.B.; Sirringhaus, H.; et al. Chalcogenophene Comonomer Comparison in Small Band Gap Diketopyrrolopyrrole-Based Conjugated Polymers for High-Performing Field-Effect Transistors and Organic Solar Cells. *J. Am. Chem. Soc.* **2015**, *137*, 1314–1321. [CrossRef]

30. Liao, S.H.; Jhuo, H.J.; Cheng, Y.S.; Chen, S.A. Fullerene Derivative-Doped Zinc Oxide Nanofilm as the Cathode of Inverted Polymer Solar Cells with Low-Bandgap Polymer (PTB7-Th) for High Performance. *Adv. Mater.* **2013**, *25*, 1314–1321. [CrossRef]

31. Yuan, J.; Zhang, Y.; Zhou, L.; Zhang, G.; Yip, H.L.; Lau, T.K.; Lu, X.; Zhu, C.; Peng, H.; Johnson, P.A.; et al. Single-Junction Organic Solar Cell with over 15% Efficiency Using Fused-Ring Acceptor with Electron-Deficient Core. *Joule* **2019**, *3*, 1140–1151. [CrossRef]

32. Ma, L.; Zhang, S.; Zhu, J.; Wang, J.; Ren, J.; Zhang, J.; Hou, J. Completely Non-Fused Electron Acceptor with 3D-Interpenetrated Crystalline Structure Enables Efficient and Stable Organic Solar Cell. *Nat. Commun.* **2021**, *12*, 5093. [CrossRef]

33. Cui, Y.; Yao, H.; Zhang, J.; Zhang, T.; Wang, Y.; Hong, L.; Xian, K.; Xu, B.; Zhang, S.; Peng, J.; et al. Over 16% Efficiency Organic Photovoltaic Cells Enabled by a Chlorinated Acceptor with Increased Open-Circuit Voltages. *Nat. Commun.* **2019**, *10*, 2515. [CrossRef] [PubMed]

34. Cheng, P.; Yang, Y. Narrowing the Band Gap: The Key to High-Performance Organic Photovoltaics. *Acc. Chem. Res.* **2020**, *53*, 1218–1228. [CrossRef] [PubMed]

35. Wang, H.; Cao, J.; Yu, J.; Zhang, Z.; Geng, R.; Yang, L.; Tang, W. Molecular Engineering of Central Fused-Ring Cores of Non-Fullerene Acceptors for High-Efficiency Organic Solar Cells. *J. Mater. Chem. A Mater.* **2019**, *7*, 4313–4333. [CrossRef]

36. Wang, K.; Li, Y.; Li, Y. Challenges to the Stability of Active Layer Materials in Organic Solar Cells. *Macromol. Rapid Commun.* **2020**, *41*, 1900437. [CrossRef] [PubMed]

37. Burgués-Ceballos, I.; Lucera, L.; Tiwana, P.; Ocytko, K.; Tan, L.W.; Kowalski, S.; Snow, J.; Pron, A.; Bürckstümmer, H.; Blouin, N.; et al. Transparent Organic Photovoltaics: A Strategic Niche to Advance Commercialization. *Joule* **2021**, *5*, 2261–2272. [CrossRef]

38. Xu, S.; Wang, W.; Liu, H.; Yu, X.; Qin, F.; Luo, H.; Zhou, Y.; Li, Z. A New Diazabenzo[k]Fluoranthene-Based D-A Conjugated Polymer Donor for Efficient Organic Solar Cells. *Macromol. Rapid Commun.* **2022**, *43*, e2200276. [CrossRef]

39. Zhang, Y.; Zhou, P.; Wang, J.; Zhan, X.; Chen, X. Designing a Thiophene-Fused Quinoxaline Unit to Build D–A Copolymers for Non-Fullerene Organic Solar Cells. *Dye. Pigment.* **2020**, *174*, 108022. [CrossRef]

40. Chen, L.; Zeng, M.; Tang, X.; Weng, C.; Tan, S.; Shen, P. Development of A-DA′D-A Small-Molecular Acceptors Based on a 6,12-Dihydro-Diindolo[1,2-b:10,20-e]Pyrazine Unit for Efficient As-Cast Polymer Solar Cells. *J. Phys. Chem. C* **2020**, *124*, 21366–21377. [CrossRef]

41. Lu, B.; Zhang, Z.; Wang, J.; Cai, G.; Wang, J.; Yuan, X.; Ding, Y.; Wang, Y.; Yao, Y. Nonfullerene Electron Acceptors with Electron-Deficient Units Containing Cyano Groups for Organic Solar Cells. *Mater. Chem. Front.* **2021**, *5*, 5549–5572. [CrossRef]

42. Jia, Z.; Qin, S.; Meng, L.; Ma, Q.; Angunawela, I.; Zhang, J.; Li, X.; He, Y.; Lai, W.; Li, N.; et al. High Performance Tandem Organic Solar Cells via a Strongly Infrared-Absorbing Narrow Bandgap Acceptor. *Nat. Commun.* **2021**, *12*, 178. [CrossRef]

43. Cheng, H.W.; Zhao, Y.; Yang, Y. Toward High-Performance Semitransparent Organic Photovoltaics with Narrow-Bandgap Donors and Non-Fullerene Acceptors. *Adv. Energy Mater.* **2022**, *12*, 2102908. [CrossRef]

44. Wei, Q.; Zhang, Y.; Shan, T.; Zhong, H. A Near-Infrared Polymer Enables over 50% Transmittance in Semi-Transparent Organic Solar Cells. *J. Mater. Chem. C Mater.* **2022**, *10*, 5887–5895. [CrossRef]

45. Babu, N.S. Studies of New 2,7-Carbazole (CB) Based Donor-Acceptor-Donor (D-A-D) Monomers as Possible Electron Donors in Polymer Solar Cells by DFT and TD-DFT Methods. *ChemistryOpen* **2022**, *11*, e202100273. [CrossRef]

46. Park, S.H.; Ahn, J.-S.; Kwon, N.Y.; Diem, C.H.; Harit, A.K.; Woo, H.Y.; Cho, M.J.; Choi, D.H. Effect of Fused Thiophene Bridges on the Efficiency of Non-Fullerene Polymer Solar Cells Made with Conjugated Donor Copolymers Containing Alkyl Thiophene-3-Carboxylate. *Macromol. Res.* **2021**, *29*, 435–442. [CrossRef]

47. Zhu, X.; Zhang, Y.; Xie, B.; Miao, J.; Ma, W.; Liu, J.; Wang, L. All-Fused-Ring Small Molecule Acceptors with near-Infrared Absorption. *J. Mater. Chem. C Mater.* **2023**, *11*, 2144–2152. [CrossRef]

48. Li, X.; Weng, K.; Ryu, H.S.; Guo, J.; Zhang, X.; Xia, T.; Fu, H.; Wei, D.; Min, J.; Zhang, Y.; et al. Non-Fullerene Organic Solar Cells Based on Benzo[1,2-b:4,5-B′]Difuran-Conjugated Polymer with 14% Efficiency. *Adv. Funct. Mater.* **2020**, *30*, 1906809. [CrossRef]

49. Li, X.; Duan, X.; Liang, Z.; Yan, L.; Yang, Y.; Qiao, J.; Hao, X.; Zhang, C.; Zhang, J.; Li, Y.; et al. Benzo[1,2-b:4,5-B′]Difuran Based Polymer Donor for High-Efficiency (>16%) and Stable Organic Solar Cells. *Adv. Energy Mater.* **2022**, *12*, 2103684. [CrossRef]

50. Al-Isaee, S.; Iraqi, A.; Lidzey, D. Synthesis and Characterisation of a New Series of 2,6-Linked-Anthracene–Benzothiadiazole Based Polymers for Organic Solar Cells Applications. *Tetrahedron* **2023**, *138*, 133416. [CrossRef]

51. Liao, C.; Gong, Y.; Xu, X.; Yu, L.; Li, R.; Peng, Q. Cost-Efficiency Balanced Polymer Acceptors Based on Lowly Fused Dithienopy-rrolo[3, 2b]Benzothiadiazole for 16.04% Efficiency All-Polymer Solar Cells. *Chem. Eng. J.* **2022**, *435*, 134862. [CrossRef]

52. Krassas, M.; Polyzoidis, C.; Tzourmpakis, P.; Kosmidis, D.M.; Viskadouros, G.; Kornilios, N.; Charalambidis, G.; Nikolaou, V.; Coutsolelos, A.G.; Petridis, K.; et al. Benzothiadiazole Based Cascade Material to Boost the Performance of Inverted Ternary Organic Solar Cells. *Energies* **2020**, *13*, 450. [CrossRef]

53. Zuo, K.; Dai, T.; Guo, Q.; Wang, Z.; Zhong, Y.; Mengzhen, D.; Wang, H.; Tang, A.; Zhou, E. PTB7-Th-Based Organic Photovoltaic Cells with a High VOCof over 1.0 v via Fluorination and Side Chain Engineering of Benzotriazole-Containing Nonfullerene Acceptors. *ACS Appl. Mater. Interfaces* **2022**, *14*, 18764–18772. [CrossRef]

54. Chen, Y.; Chen, F. Fluorination Effects on Bithiophene Unit in Benzodithiophene-4,8-Dione Based D-A Type Alternating Copoly-mers for Highly Efficient Polymer Solar Cells. *RSC Adv.* **2022**, *12*, 36038–36045. [CrossRef]

55. Duan, L.; Uddin, A. Progress in Stability of Organic Solar Cells. *Adv. Sci.* **2020**, *7*, 1903259. [CrossRef]

56. Tetreault, A.R.; Dang, M.T.; Bender, T.P. PTB7 and PTB7-Th as Universal Polymers to Evaluate Materials Development Aspects of Organic Solar Cells Including Interfacial Layers, New Fullerenes, and Non-Fullerene Electron Acceptors. *Synth. Met.* **2022**, *287*, 117088. [CrossRef]

57. Zhong, H.; Ye, L.; Chen, J.Y.; Jo, S.B.; Chueh, C.C.; Carpenter, J.H.; Ade, H.; Jen, A.K.Y. A Regioregular Conjugated Polymer for High Performance Thick-Film Organic Solar Cells without Processing Additive. *J. Mater. Chem. A Mater.* **2017**, *5*, 10517–10525. [CrossRef]

58. Huang, X.; Zhang, L.; Cheng, Y.; Oh, J.; Li, C.; Huang, B.; Zhao, L.; Deng, J.; Zhang, Y.; Liu, Z.; et al. Novel Narrow Bandgap Terpolymer Donors Enables Record Performance for Semitransparent Organic Solar Cells Based on All-Narrow Bandgap Semiconductors. *Adv. Funct. Mater.* **2022**, *32*, 2108634. [CrossRef]

59. Lee, J.; Cha, H.; Yao, H.; Hou, J.; Suh, Y.H.; Jeong, S.; Lee, K.; Durrant, J.R. Toward Visibly Transparent Organic Photovoltaic Cells Based on a Near-Infrared Harvesting Bulk Heterojunction Blend. *ACS Appl. Mater. Interfaces* **2020**, *12*, 32764–32770. [CrossRef]

60. Xie, Y.; Cai, Y.; Zhu, L.; Xia, R.; Ye, L.; Feng, X.; Yip, H.L.; Liu, F.; Lu, G.; Tan, S.; et al. Fibril Network Strategy Enables High-Performance Semitransparent Organic Solar Cells. *Adv. Funct. Mater.* **2020**, *30*, 2002181. [CrossRef]

61. Hu, Z.; Wang, Z.; An, Q.; Zhang, F. Semitransparent Polymer Solar Cells with 12.37% Efficiency and 18.6% Average Visible Transmittance. *Sci. Bull.* **2020**, *65*, 131–137. [CrossRef]
62. Yoon, J.W.; Bae, H.; Yang, J.; Ha, J.W.; Lee, C.; Lee, J.; Yoon, S.C.; Choi, H.; Ko, S.J. Semitransparent Organic Solar Cells with Light Utilization Efficiency of 4% Using Fused-Cyclopentadithiophene Based near-Infrared Polymer Donor. *Chem. Eng. J.* **2023**, *452*, 139423. [CrossRef]
63. Jiang, T.; Zhang, G.; Xia, R.; Huang, J.; Li, X.; Wang, M.; Yip, H.L.; Cao, Y. Semitransparent Organic Solar Cells Based on All-Low-Bandgap Donor and Acceptor Materials and Their Performance Potential. *Mater. Today Energy* **2021**, *21*, 100807. [CrossRef]
64. Wang, J.; Xue, P.; Jiang, Y.; Huo, Y.; Zhan, X. The Principles, Design and Applications of Fused-Ring Electron Acceptors. *Nat. Rev. Chem.* **2022**, *6*, 614–634. [CrossRef]
65. Yang, Y. The Original Design Principles of the Y-Series Nonfullerene Acceptors, from Y1 to Y6. *ACS Nano* **2021**, *15*, 18679–18682. [CrossRef]
66. Yao, H.; Chen, Y.; Qin, Y.; Yu, R.; Cui, Y.; Yang, B.; Li, S.; Zhang, K.; Hou, J. Design and Synthesis of a Low Bandgap Small Molecule Acceptor for Efficient Polymer Solar Cells. *Adv. Mater.* **2016**, *28*, 8283–8287. [CrossRef]
67. Hu, Z.; Wang, Z.; Zhang, F. Semitransparent Polymer Solar Cells with 9.06% Efficiency and 27.1% Average Visible Transmittance Obtained by Employing a Smart Strategy. *J. Mater. Chem. A Mater.* **2019**, *7*, 7025–7032. [CrossRef]
68. Yao, H.; Cui, Y.; Yu, R.; Gao, B.; Zhang, H.; Hou, J. Design, Synthesis, and Photovoltaic Characterization of a Small Molecular Acceptor with an Ultra-Narrow Band Gap. *Angew. Chem.-Int. Ed.* **2017**, *56*, 3045–3049. [CrossRef]
69. Chen, J.; Li, G.; Zhu, Q.; Guo, X.; Fan, Q.; Ma, W.; Zhang, M. Highly Efficient Near-Infrared and Semitransparent Polymer Solar Cells Based on an Ultra-Narrow Bandgap Nonfullerene Acceptor. *J. Mater. Chem. A Mater.* **2019**, *7*, 3745–3751. [CrossRef]
70. Li, Y.; Guo, X.; Peng, Z.; Qu, B.; Yan, H.; Ade, H.; Zhang, M.; Forrest, S.R. Color-Neutral, Semitransparent Organic Photovoltaics for Power Window Applications. *Proc. Natl. Acad. Sci. USA* **2020**, *117*, 21147–21154. [CrossRef]
71. Zhang, Y.; Wei, Q.; He, Z.; Wang, Y.; Shan, T.; Fu, Y.; Guo, X.; Zhong, H. Efficient Optoelectronic Devices Enabled by Near-Infrared Organic Semiconductors with a Photoresponse beyond 1050 Nm. *ACS Appl. Mater. Interfaces* **2022**, *14*, 31066–31074. [CrossRef]
72. Xu, X.; Wei, Q.; Zhou, Z.; He, H.; Tian, J.; Yip, H.L.; Fu, Y.; Lu, X.; Zhou, Y.; Li, Y.; et al. Efficient Semitransparent Organic Solar Cells with CRI over 90% Enabled by an Ultralow-Bandgap A-DA'D-A Small Molecule Acceptor. *Adv. Funct. Mater.* **2023**. *early view*. [CrossRef]
73. Zhu, J.; Hao, R.; Wang, J.; Sun, D.; Song, X.; Zhu, M.; Zhang, B.; Liu, Y.; Tan, H.; Zhu, W. Boosting Efficiency and Stability for Organic Solar Cells by Subtle Management Electron-Withdrawing Terminal of Electron Acceptors Based on Asymmetric Dual-Donor Centra. *Dye. Pigment.* **2023**, *210*, 111003. [CrossRef]
74. Wang, Y.; Luke, J.; Privitera, A.; Rolland, N.; Labanti, C.; Londi, G.; Lemaur, V.; Toolan, D.T.W.; Sneyd, A.J.; Jeong, S.; et al. The Critical Role of the Donor Polymer in the Stability of High-Performance Non-Fullerene Acceptor Organic Solar Cells. *Joule* **2023**, *7*, 810–829. [CrossRef]
75. Liu, B.; Sun, H.; Lee, J.W.; Jiang, Z.; Qiao, J.; Wang, J.; Yang, J.; Feng, K.; Liao, Q.; An, M.; et al. Efficient and Stable Organic Solar Cells Enabled by Multicomponent Photoactive Layer Based on One-Pot Polymerization. *Nat. Commun.* **2023**, *14*, 967. [CrossRef]
76. Zhang, Z.; Miao, J.; Ding, Z.; Kan, B.; Lin, B.; Wan, X.; Ma, W.; Chen, Y.; Long, X.; Dou, C.; et al. Efficient and Thermally Stable Organic Solar Cells Based on Small Molecule Donor and Polymer Acceptor. *Nat. Commun.* **2019**, *10*, 3271. [CrossRef]
77. Li, Y.; Liu, K.-K.; Lin, F.R.; Jen, A.K.-Y. Improving the Stability of Organic Solar Cells: From Materials to Devices. *Sol. RRL* **2023**, *7*, 2300531. [CrossRef]
78. Tu, S.; Lin, X.; Xiao, L.; Zhen, H.; Wang, W.; Ling, Q. Boosting the Overall Stability of Organic Solar Cells by Crosslinking Vinyl-Functionalized Polymer Derived from PM6. *Mater. Chem. Front.* **2022**, *6*, 1150–1160. [CrossRef]